Quantum Memristors

P. Pfeiffer,[1] I. L. Egusquiza,[2] M. Di Ventra,[3] M. Sanz,[1] and E. Solano[1,4]

[1]*Department of Physical Chemistry, University of the Basque Country UPV/EHU, Apartado 644, E-48080 Bilbao, Spain*
[2]*Department of Theoretical Physics and History of Science, University of the Basque Country UPV/EHU, Apartado 644, E-48080 Bilbao, Spain*
[3]*Department of Physics, University of California, San Diego, La Jolla, CA 92093, USA*
[4]*IKERBASQUE, Basque Foundation for Science, Maria Diaz de Haro 3, 48013 Bilbao, Spain*

(Dated: November 9, 2015)

Technology based on memristors, resistors with memory whose resistance depends on the history of the crossing charges, has lately enhanced the classical paradigm of computation with neuromorphic architectures. However, in contrast to the known quantized models of passive circuit elements, such as inductors, capacitors or resistors, the design and realization of a quantum memristor is still missing. Here, we introduce the concept of a quantum memristor as a quantum dissipative device, whose decoherence mechanism is controlled by a continuous-measurement feedback scheme, which accounts for the memory. Indeed, we provide numerical simulations showing that memory effects actually persist in the quantum regime. Our quantization method, specifically designed for superconducting circuits, may be extended to other quantum platforms, allowing for memristor-type constructions in different quantum technologies. The proposed quantum memristor is then a building block for neuromorphic quantum computation and quantum simulations of non-Markovian systems.

arXiv:1511.02192v1 [quant-ph] 6 Nov 2015

Although they are often misused terms, the difference between information storage and memory is relevant. While the former refers to save information in a physical device for a future use without changes, a physical system shows memory when its dynamics, usually named non-Markovian [1, 2], depend on the past states of the system. Recently, there is a growing interest in memristors, resistors with history-dependent resistance which provide memory effects in form of a resistive hysteresis [3, 4]. In this sense, memristors, due to their memory capabilities [5–7], offer novel applications in information processing architectures.

A classical memristor is a resistor whose resistance depends on the record of the electrical signals, namely voltage or charges, applied to it. The information about the electrical history is contained in the physical configuration of the memristor, summarized in its internal state variable μ, which enters the (voltage-controlled) memristor I-V-relationship via [8],

$$I(t) = G(\mu(t))V(t), \tag{1a}$$
$$\dot{\mu}(t) = f(\mu(t), V(t)). \tag{1b}$$

The state variable dynamics, encoded in the real-valued function $f(\mu(t), V(t))$ and the state variable-dependent conductance function $G(\mu(t)) > 0$, leads to a characteristic pinched hysteresis loop of a memristor under a periodic driving.

In superconducting circuits, electrical signals are quantized and can be used to implement quantum simulations [9, 10], perform quantum information tasks [11], or quantum computing [12, 13]. However, despite its prospects in classical information processing, memristors have not been considered so far in quantized circuits. The quantum regime of electrical signals is accessed by operating superconducting electric circuits at cryogenic temperatures. Their behavior is well-described by canonical quantization of Lagrange models that reproduce the classical circuit dynamics [14]. Furthermore, the effects of dissipative elements like conventional resistors are studied by coupling the circuit to environmental degrees of freedom represented by a transmission line [15] or a bath of harmonic oscillators [16]. Yet, previous studies of memory elements in quantized circuits focussed only on non-dissipative components like memcapacitors and meminductors. This is due to the fact that the history-dependent damping requires dissipative potentials, which cannot be cast in simple system-environment frames [17].

In this Letter, we propose a design of a quantum memristor, closing the gap left by the classical memristor in the quantization toolbox for circuits [18]. Equation (1b) can be understood as an information extraction process and, hence, its effect may be modeled on a circuit by continuous measurements. Furthermore, the state-dependent resistance in Eq. (1a) is mimicked by a measurement-controlled coupling between the circuit and a bath of harmonic oscillators. Hence, our model for a quantum memristor constitutes a special case of quantum feedback control [19], which is not restricted to superconducting circuits. As a paradigmatic example of a quantum memristor, we study a quantum LC circuit shunted by a memristor (see Fig. 1a), and address the compatibility between memory effects and quantum properties like coherent superpositions.

Quantum memristor dynamics – We decompose the influence of a quantum memristor on the system into a Markovian tunable dissipative environment, a weak-measurement protocol, and a classical feedback controlling the coupling of the system to the dissipative environment. Then, the evolution of the circuit quantum state ρ includes a back action term due to the presence of the weak measurements. In addition, the dynamics contains a dissipative contribution, which depends on the state variable μ, and a Hamiltonian part, so that

$$\mathrm{d}\rho = \mathrm{d}\rho_H + \mathrm{d}\rho_{meas} + \mathrm{d}\rho^{(\mu)}_{damp}, \tag{2}$$

which essentially plays the role of Eq. (1a). Correspondingly, if the interaction between the state variable and the circuit is cast in a measurement, the voltage records $M_V(t)$ govern the

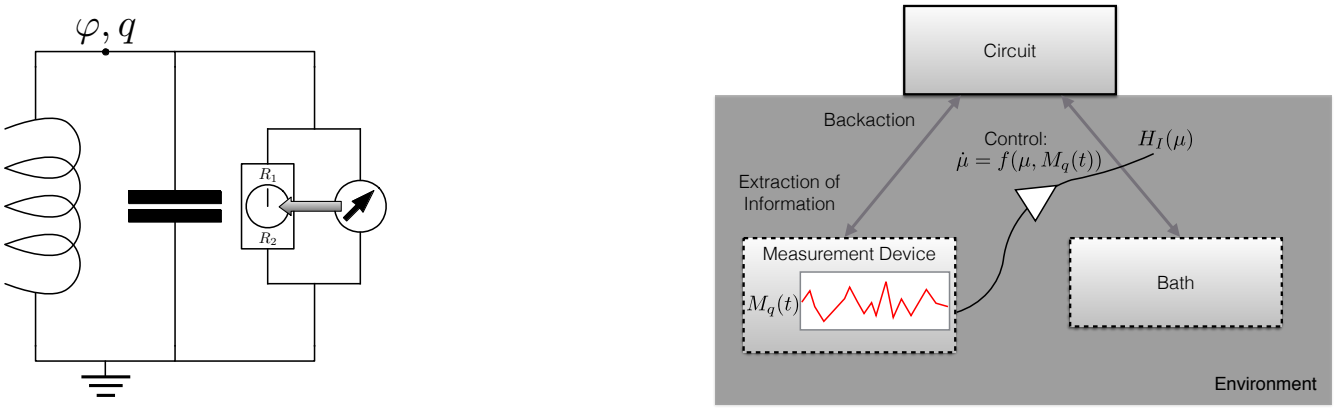

(a) Shunted LC circuit

(b) Feedback model

FIG. 1. **(a)** Scheme of an LC circuit shunted by a memristor, which following our scheme, it is replaced by a tunable dissipative ohmnic environment, a weak-measurement protocol, and a feedback tuning the coupling of the dissipative environment depending on the measurement outcome. **(b)** Feedback model of a memristor and implementation in quantum dynamics via a feedback-controlled open quantum system.

state variable dynamics,

$$\dot{\mu}(t) = f(\mu(t), M_V(t)). \tag{3}$$

Finally, the Hamiltonian part is determined by the circuit structure. In the following, we illustrate the method by shunting an LC circuit with a quantum memristor, as depicted in Fig. 1. Its description requires only one degree of freedom, the top node flux φ, and its conjugate momentum q [14], which corresponds to the charge on the capacitor connected to the top node. Therefore, we have

$$\mathrm{d}\rho_H = -\frac{i}{\hbar}\left[H(\varphi, q), \rho(t)\right]\mathrm{d}t\,. \tag{4}$$

The measurement of the voltage applied to the quantum memristor implies a monitoring of the node charge q, since the voltage determines the charge on the capacitor with capacitance C, $q = CV$. Therefore, according to the theory of continuous measurements [19, 20], the state update and the measurement output have respectively the form

$$\begin{aligned}\mathrm{d}\rho_{meas} = &-\frac{\tau}{q_0^2}\left[q, [q, \rho(t)]\right]\mathrm{d}t \\ &+\sqrt{\frac{2\tau}{q_0^2}}\left(\{q, \rho(t)\} - 2\langle q\rangle \rho(t)\right)\mathrm{d}W, \end{aligned} \tag{5a}$$

$$M_V(t) = \frac{1}{C}\left(\langle q(t)\rangle + \sqrt{\frac{q_0^2}{8\tau}}\zeta(t)\right), \tag{5b}$$

where $\{A, B\} = AB + BA$ is the anticommutator and the mean value of an observable reads $\langle A\rangle = \mathrm{Tr}\,(\rho A)$. The projection frequency τ is defined as the inverse of the measurement time needed to determine the mean charge up to an uncertainty q_0, and depends on the measurement strength $k = \frac{\tau}{q_0^2}$. In the limit $\tau \to \infty$, we recover the usual projective measurement. On the other hand, in the limit $\tau \to 0$, the measurement apparatus is decoupled from the system, obtaining no information about it. Finally, the stochasticity of the measurement output enters via the white noise $\zeta(t)$, and the Wiener increment $\mathrm{d}W$ induces the corresponding probabilistic update of the quantum state.

A constant resistor with resistance R can be simulated by a bath of LC circuits with an ohmic spectral density [14],

$$J_{ohm}(\omega) = \frac{2C\gamma}{\pi}\omega\frac{\Omega^2}{\Omega^2 + \omega^2}. \tag{6}$$

Here, the relaxation rate of the circuit is $\gamma = \frac{1}{2RC}$ and Ω denotes a cut-off frequency. In the high temperature and high cut-off frequency limit, $\lambda := \frac{k_B T}{\hbar}, \Omega \gg \omega_0$, with ω_0 the typical circuit frequency, the dissipative contribution to the circuit dynamics can be cast in the Caldeira-Leggett (C-L) master equation [1, 16]. In a sufficiently small time slice $\mathrm{d}t$, in which μ remains approximately constant, a quantum memristor acts like a resistor with resistance $G(\mu)^{-1}$. Therefore, we adapt the C-L form by replacing the constant relaxation rate γ by a function $\gamma(\mu) = \frac{G(\mu)}{2C}$,

$$\begin{aligned}\mathrm{d}\rho_{damp}^{\gamma(\mu)} = &-\frac{i\gamma(\mu)}{\hbar}\left[\varphi, \{q, \rho(t)\}\right]\mathrm{d}t \\ &-\frac{2C\lambda\gamma(\mu)}{\hbar}\left[\varphi, [\varphi, \rho(t)]\right]\mathrm{d}t. \end{aligned} \tag{7}$$

This phenomenological form could in principle be verified in a two-step procedure. Firstly, by capturing the full joint dynamics of the circuit and the bath when subjected to a feedback control of their interaction Hamiltonian. Secondly, by extracting the circuit dynamics after tracing out the bath degrees of freedom, as depicted in Fig. 1b. However, the required feedback is non-Markovian, i.e. comprises voltage values from the past, and these systems are generally not analytically tractable [19]. Still, the C-L form represents a plausible choice, if the ordering $t_{relax} \ll t_{control} \ll t_{exchange} \ll \mathrm{d}t$

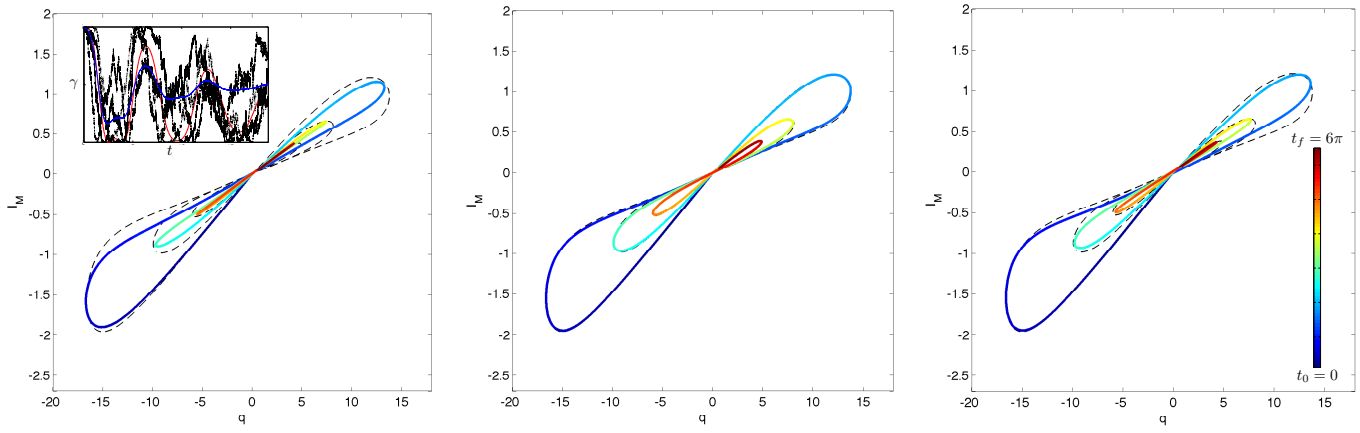

(a) $\tau = 0.005$ (b) $\tau = 0.2$ (c) $\tau = 4$

FIG. 2. Hysteresis plots of the memristor for the unconditioned evolution with increasing projection frequencies τ. The comparison with the classical hysteresis curve (black, dashed) shows the collapse in the case of a very strong or very weak measurement. The inset shows the evolution of the damping rate and depict several of the underlying stochastic trajectories corresponding to one realisation of the conditioned dynamics. The parameters are $\gamma_0 = 0.1, \epsilon = 0.5, \lambda = 10, \nu = 0.1$, the initial conditions are $\langle\varphi\rangle(0) = 20, \langle q\rangle(0) = 0, V_\varphi = 0.5, V_q = 0.5, C_{\varphi,q} = 0, \mu(0) = 0$ and the average was obtained by generating 3000 trajectories of the stochastic dynamics via the Euler algorithm with $\mathrm{d}t = 10^{-3}$

holds for a time-coarse graining (See Supplementary material for a detailed argumentation).

Consider now an observer that has no access to the measurement output $M_V(t)$. From the observer's point of view, the system evolves with density matrix $\bar{\rho} = \langle\langle\rho\rangle\rangle$, where $\langle\langle\cdot\rangle\rangle$ denotes the average over all realizations of the Wiener noise. We shall use the term *unconditioned state* to refer to $\bar{\rho}$. The evolution of the unconditioned state is determined by the ensemble average of Eq. (2). Clearly, we do not generally obtain a closed system for $\bar{\rho}$ since $\langle\langle\gamma(\mu)\rho\rangle\rangle$, which appears in the ensemble average of the dissipative term, does not in principle factorize. Now, when it does factorize and $\langle\langle\gamma(\mu)\rangle\rangle$ is constant, the evolution equation of $\bar{\rho}$ is of Lindblad form, describing a memoryless quantum Markov process. Thus, it provides us with a witness for non-Markovianity.

To sum up, the quantum-memristor dynamics given by increments of the quantum state in Eqs. (4), (5a) and (7), together with the state variable update in Eq. (3), evolves via two coupled, non-linear stochastic differential equations. Their form is designed to mimic the memory effect due to a memristor, by means of a damping rate which depends on partial information of the history of the quantum state. Unfortunately, this complex dynamics prevents an analytical approach, so we treat it numerically.

Hysteresis in a quantum memristor – We present a numerical study of the dynamics of Gaussian states in an LC circuit shunted by a quantum memristor with linear state variable dynamics and the memristance of a Josephson junction [21]. For convenience, charge and flux are expressed in units of their vacuum fluctuations, $\varphi_0 = \sqrt{\frac{\hbar}{\omega_0 C}}$ and $q_0 = \sqrt{\hbar\omega_0 C}$, with C the capacitance. Furthermore, frequency is expressed in units of the circuit frequency $\omega_0 = \frac{1}{\sqrt{LC}}$, where L is the inductance of the coil. Hence, the Hamiltonian reads

$$H = \frac{\hbar}{2}(q^2 + \varphi^2).$$

This quadratic Hamiltonian, as well as the damping and the measurement contribution to the dynamics, preserve the Gaussianity of an initial state. Therefore, it suffices to follow the evolution of the first and second moments of flux and charge [22], which together with the damping function $\gamma(\mu)$ and the state variable dynamics, fully determine the dynamics of the conditioned state ρ (see [20]),

$$\mathrm{d}\langle\varphi\rangle = \langle q\rangle\,\mathrm{d}t + \sqrt{8\tau}C_{\varphi,q}\mathrm{d}W, \tag{8a}$$

$$\mathrm{d}\langle q\rangle = -\langle\varphi\rangle\,\mathrm{d}t - 2\gamma(\mu)\langle q\rangle\,\mathrm{d}t + \sqrt{8\tau}V_q\mathrm{d}W, \tag{8b}$$

$$\mathrm{d}V_\varphi = 2C_{\varphi,q}\mathrm{d}t + 2\tau(1 - 4C_{\varphi,q}^2)\mathrm{d}t, \tag{8c}$$

$$\mathrm{d}V_q = -2C_{\varphi,q}\mathrm{d}t - 4\gamma(\mu)(V_q - \lambda)\,\mathrm{d}t - 8\tau V_q^2\mathrm{d}t, \tag{8d}$$

$$\mathrm{d}C_{\varphi,q} = (V_q - V_\varphi)\mathrm{d}t - C_{\varphi,q}(2\gamma(\mu) + 8\tau V_q)\mathrm{d}t, \tag{8e}$$

$$\mathrm{d}\mu = \nu\left(\langle q\rangle\,\mathrm{d}t + \frac{\mathrm{d}W}{\sqrt{8\tau}}\right), \tag{8f}$$

$$\gamma(\mu) = \gamma_0(1 + \epsilon\cos(\mu)). \tag{8g}$$

The frequency ν determines the rate of change of the state variable per unit of charge q_0. If the unitless feedback parameter $\epsilon \in [0, 1]$ vanishes, the damping rate equals the constant γ_0, and the system reduces to an LC circuit coupled to a constant resistor and a voltmeter.

The set of Eqs. (8) depends on the projection frequency τ, which is a free parameter, since it is not determined by Eqs. (1). Indeed, if we consider the classical limit corresponding to charging the capacitor for $\langle q\rangle \to \infty$, we recover Eqs. (1) for every positive τ. Therefore, there is an infinite family of quantum memristors producing the same classical memristive dynamics. However, in the low charging regime, the area

of the hysteresis loop in the I-V-characteristic of the quantum memristor in the unconditioned evolution changes with τ. As the voltage is proportional to the charge on the capacitor and the conductance is proportional to the damping, to obtain the hysteresis loop means to plot $\langle\langle V\rangle\rangle \propto \langle\langle q\rangle\rangle$ vs. $\langle\langle I_M\rangle\rangle = \langle\langle\gamma(\mu)q\rangle\rangle$. From the set of Eqs. (8), two sources of diffusion of the state variable μ can be identified, namely, the noisy measurement output and the stochastic back-action on the first moments (terms in Eqs. (8a), (8b), and (8f) proportional to the Wiener increment $\mathrm{d}W$). These diffusive terms reduce the hysteresis area, since their physical origins, statistical averaging over multiple voltage histories and respectively, insufficient information extraction, counteract memory effects. Indeed, once the state variable is spread over a range $\geq 2\pi$, the periodicity of the damping rate function leads to a stationary value of its ensemble average, $\langle\langle\gamma\rangle\rangle = \gamma_0$, and the hysteresis loop collapses.

In Fig. 2, the successive collapse of the hysteresis for a strong and a weak measurement case is contrasted with the classical hysteresis, which almost coincides with the hysteresis for the optimal choose of τ, balancing information gain and measurement back-action (cf. Supplementary Material).

According to our model, the dynamics of the quantum LC circuit has acquired a non-Markovian character by coupling it to a quantum memristor. The question remains, whether characteristics of a genuine quantum system like coherent superpositions are affected by the memristive environment. The existence of non-linear terms in Eqs. (8), which in principle destroy the coherence of the superpositions, makes nontrivial the answer to this question. In any case, one must understand this non-linear behavior as the *effective* action of the environment-measurement-feedback protocol, i. e. the quantum memristor, onto the system. This paves the way for employing these quantum memristors as a natural building block for simulating non-linear dynamics or designing non-linear dissipative gates. In particular, and in view of the success of the classical memristor proposal [5, 6], this opens the door to a possible development of neuromorphic architectures for quantum computing.

Similarly, one may wonder about the quantumness of the quantum memristor dynamics. Numerically, one can observe oscillations in the squeezing of the quantum state, so that an initial Gaussian state, whose variance is squeezed in momentum V_q, periodically changes its squeezing to space, V_φ, during the evolution. In other words, the system density matrix does not commute with itself for different times, which is an evidence of the quantumness of the dynamics.

Even though the idea of engineering memristors in the quantum realm seems cumbersome, there are already proposals for employing the memristive component of the Josephson junctions in an asymmetric SQUID in superconducting qubits [21]. Unfortunately, the quantization of the proposed design is not complete, since it is described by a semiclassical model. At any rate, it shows that the idea of a quantum memristor is experimentally feasible.

Conclusion – We have introduced quantum memristors and presented a protocol to construct properly the evolution equation for superconducting circuits coupled to quantum memristors. Our model is not restricted to electric circuits and could also be investigated in other quantum platforms like trapped ions or quantum photonics. Besides, we have constructively demonstrated the non-Markovian character of the quantum memristor dynamics, which allowed us to conjecture that the memory effects measured as the area of the hysteresis loop are maximized in the classical limit. Due to the impressive features shown by novel memristor-based computer architectures [5, 6, 29], the quantum memristors proposed here may be considered as a building block for neuromorphic quantum computation and quantum simulation of non-Markovian systems.

ACKNOWLEDGEMENTS

We would like to acknowledge support from Spanish MINECO grant FIS2012-36673-C03-02, Basque Government grants IT-472-10 and IT-559-10, UPV/EHU grant UFI 11/55, PROMISCE and SCALEQIT EU projects. E. S. also acknowledges support from a TUM August-Wilhelm Scheer Visiting Professorship and hospitality of Walther-Meiner-Institut and TUM Institute for Advanced Study. M. D. acknowledges partial support from DOE grant DE-FG02-05ER46204.

[1] H.-P. Breuer and F. Petruccione, *The Theory of Open Quantum Systems* (Oxford University Press, 2007).
[2] C. Gardiner, *Stochastic Methods: A Handbook for the Natural and Social Sciences* (Springer Berlin Heidelberg, 2010).
[3] L. Chua, IEEE Transactions on Circuit Theory, pp.507519 (1971).
[4] D.B. Strukov, G.S. Snider, D.R. Stewart, R.S. Williams, Nature **453**, 7191 (2008).
[5] F. L. Traversa and M. Di Ventra, IEEE Trans. Neur. Networks and Learn. Sys. **26**, 2702 (2015).
[6] F. L. Traversa, C. Ramella, F. Bonani, and M. di Ventra, Sci. Adv **1**, 5 (2015).
[7] J.J. Yang, D.B. Strukov, D.R. Stewart, Nature Nanotechnology **8**, 1 (2013).
[8] M. Di Ventra, Y. V. Pershin, Nanotechnology **24**, 25 (2013).
[9] Y. Salathé et al., Phys. Rev. X **5**, 021027 (2015).
[10] R. Barends et al., Nature Commun. **6**, 7654 (2015).
[11] S. Felicetti et al. Phys. Rev. Lett. 113, 093602 (2014).
[12] R. Barends et al., Nature **508**, 500 (2015).
[13] D. Ristè et al., Nature Commun. **6**, 6983 (2015).
[14] M.H. Devoret, in *Quantum Fluctuations, Lecture Notes of the 1995 Les Houches Summer School*, edited by S. Reynaud, E. Giacobino, and J. Zinn-Justin (Elsevier, The Netherlands, 1997, p. 351).
[15] B.Yurke, J. Denker, Phys. Rev. A **29**, 3 (1984).
[16] A. Caldeira, A. Leggett, Annals of Physics **149** 2 (1983).
[17] G. Z. Cohen, Y. V. Pershin, M. Di Ventra, Physical Review B **85**,16 (2012).
[18] P. Pfeiffer, Master's Thesis, Ludwig Maximilian University, Munich, 2015

[19] H. M. Wiseman, G. J. Milburn, *Quantum Measurement and Control* (Cambridge University Press, 2010).
[20] K. Jacobs, D.A. Steck, Contemporary Physics **47**, 5 (2006).
[21] S. Peotta, M. Di Ventra, Physical Review Applied, **2**,3 (2014).
[22] The charge and flux variances are defined as $V_q = \langle q^2 \rangle - \langle q \rangle^2$, $V_\varphi = \langle \varphi^2 \rangle - \langle \varphi \rangle^2$ and the covariance reads $C_{\varphi,q} = \frac{1}{2} \langle \{\varphi, q\} \rangle - \langle \varphi \rangle \langle q \rangle$.
[23] A. Stotland, M. Di Ventra, Physical Review E, **85**,1 (2012).
[24] M. Schlosshauer, arXiv:1404.2635; *to appear in: Handbook of Quantum Information* (Springer, 2014).
[25] T. Bhattacharya, S. Habib, K. Jacobs, Physical Review Letters, **85**, 23 (2000).
[26] M. Sandberg, C. M. Wilson, F. Persson, T. Bauch, G. Johansson, V. Shumeiko, P. Delsing, Applied Physics Letters, **92**, 20 (2008).
[27] M. Pierre, I.-M. Svensson, S. Raman Sathyamoorthy, G. Johansson, P. Delsing, Applied Physics Letters, **104**,23, (2014).
[28] Y. Pershin, S. La Fontaine, M. Di Ventra, Physical Review E, **80**, 2 (2009).
[29] Tom Simonite, *IBM Making Plans to Commercialize Its Brain-Inspired Chip*, MIT Technology Review, October 15, 2015. `http://www.technologyreview.com/news/542366/ibm-making-plans-to-commercialize-its-brain-inspired-chip/`, retrieved Nov 6, 2105.

SUPPLEMENTARY MATERIAL

Time scales of the quantum memristor dynamics

The Caldeira-Leggett (C-L) model describes the dynamics of open quantum systems weakly coupled to a bath of harmonic oscillators at high temperature. Hence, it assumes, first, that the collection of harmonic oscillators is in a thermal state, and, second, that the interaction with the open system is governed by a fixed, weakly interacting Hamiltonian H_I [1].

In the model of the quantum memristor, the interaction Hamiltonian is controlled by measurement results. The output of measurements is included in Eq. (5). There is a measurement result for every interval $\mathrm{d}t$. We assume systematically that the control time $t_{control}$ that is required at each step to fully achieve the necessary tuning of the interaction Hamiltonian is small when compared to the interval $\mathrm{d}t$. Schematically, the interaction Hamiltonian does not change during intervals of length $\mathrm{d}t$ and does change during intervals of width $t_{control}$, as illustrated in Fig. 3.

We require that during most of the time interval of length $\mathrm{d}t$ the bath, and the system interaction with it, be properly described by the C-L model. As a first consequence, we need the thermal structure of the harmonic oscillator bath to be guaranteed. Therefore, the bath relaxation time scale must be shorter than the control time,

$$t_{relax} \ll t_{control}.$$

Secondly, the interaction between the system and the bath has to be determined by the values of the interaction Hamiltonian in the plateaus, and should not depend on the form of the control step. Specifically, the time during which there is exchange of excitations between open system and bath needs to be large compared to the control time,

$$t_{control} \ll t_{exchange}.$$

In this case, no excitation is exchanged during the tuning of the interaction Hamiltonian.

In summary, our working assumption is the time scale ordering shown in Fig. 3,

$$t_{relax} \ll t_{control} \ll t_{exchange} \ll \mathrm{d}t.$$

Classical hysteresis and optimal projection frequency

Classical hysteresis

The classical hysteresis curve is obtained by treating the LC circuit coupled to the quantum memristor (see Fig. 1a) classically. The second Kirchhoff's law requires the currents from the three branches, I_L (inductor), I_C (capacitor) and I_M (quantum memristor) to sum to zero, $I_L + I_C + I_M = 0$, or equivalently,

$$\frac{\Phi}{L} + \dot{Q} + G(\mu)\frac{Q}{C} = 0. \tag{9}$$

Here, the inductor flux is Φ, the charge on the capacitor is denoted by Q, and the memconductance G is a function of the state variable μ. Furthermore, the voltages across the inductor and the capacitor are the same,

$$\dot{\Phi} = \frac{Q}{C}. \tag{10}$$

Finally, the second quantum memristor equation (see Eq. (1b)) determines the evolution of the state variable μ, which in our case is a linear function of the applied voltage

$$\dot{\mu} = \nu \frac{V}{V_0} = \nu \frac{Q}{Q_0}. \tag{11}$$

Here, the role of the memory frequency ν becomes clear. It determines the rate of change of the quantum memristor state variable per unit charge Q_0 on the capacitor. Clearly, it depends on the choice of this unit charge and we chose the charge fluctuation $(\times\sqrt{2})\ q_0 = \sqrt{\hbar\omega_0 C}$ of the LC-circuit in the ground state.

In the dimensionless notation used in the main body of the paper, equations (9) , (10) and (11) read

$$\begin{aligned}
\frac{\mathrm{d}}{\mathrm{dt}}\, q(t) &= -\varphi(t) - 2\gamma(\mu(t))q(t), \\
\frac{\mathrm{d}}{\mathrm{dt}}\, \varphi(t) &= q(t), \\
\frac{\mathrm{d}}{\mathrm{dt}}\, \mu(t) &= \nu q(t).
\end{aligned}$$

On solving this set of equations, the resulting V-I_M curve shows hysteresis in the voltage-current relation of the memristor for a classical circuit. The black dotted hysteresis curves in the q-$\gamma(\mu)q$ plot in Fig. 2 correspond to such solutions, with initial conditions given by the initial expectation values of the corresponding quantum operators $q(0) = \langle q \rangle\,(0) and \varphi(0) = \langle \varphi \rangle\,(0)$, and the same initial state variable value $\mu(0) = \mu_0$.

Optimal projection frequency

In our model τ, which is the projection frequency of the measurement, is a free parameter. It measures the rate in which information is extracted by measurements in the circuit. In a physical implementation of the feedback scheme in the quantum memristor model, it would be tuned by controlling the coupling between the open system and the measurement device. In the classical limit, which corresponds to a large charge in the capacitor, the effective classical memristor equations are independent of τ.

As discussed in the main text, the projection frequency determines the information gain about the circuit variables as well as their perturbation due to the measurement. Both uncertainty in the measurement, on the one hand, and backaction, on the other, lead to diffusion of the state variable. Since the projection frequency impacts on both, an optimal τ would correspond to a measuremen, which extracts sufficient information, while inducing only small fluctuations. In other words, the optimal τ minimises the state variable variance growth.

To determine an approximation of the optimal τ we analyse the sum of the noise terms in Eq. (8),

$$D(\tau) = \sqrt{8\tau} V_q + \sqrt{8\tau}|C_{\varphi,q}| + \frac{1}{\sqrt{8\tau}}. \tag{12}$$

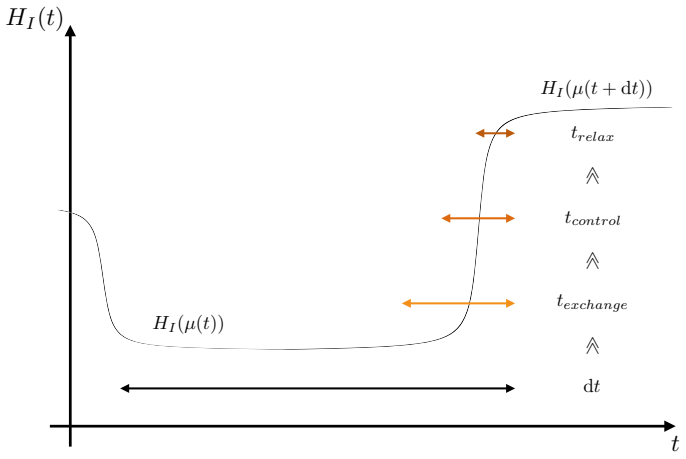

FIG. 3. Schematic tuning of the interaction Hamiltonian between bath and system. The time ordering of bath relaxation, control time and excitation exchange duration ensures the validity of the Caldeira-Leggett model in every interval $\mathrm{d}t$ of the coarse graining of time.

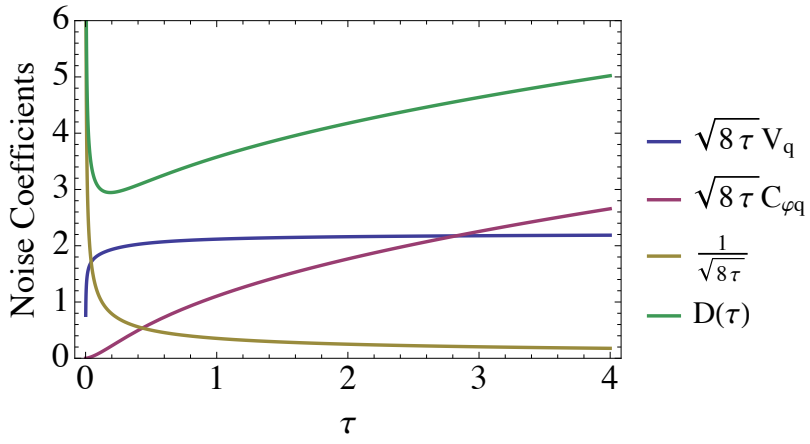

FIG. 4. Dependence of all diffusive terms in first moments and state variable on the projection frequency τ. The low noise regime suggested by this image is determined by $\tau \approx 0.2$, for the values of damping rate $\gamma = 0.1$ and thermal frequency $\lambda = 10$.

The charge variance V_q and the covariance $C_{\varphi,q}$ are a function of time, but they quickly reach quasi stationary values. There are small variations due to the changes in the damping rate γ. If we fix the damping rate at its mean value γ_0 (see Eq. 8g), the stationary values of Eq. (8d) and (8e) are

$$C^{st}_{\varphi,q} = -\frac{1}{8\tau}\left(\sqrt{1+(4\tau)^2}-1\right), \tag{13}$$

$$V^{st}_q(\tau) = \frac{\sqrt{\gamma_0^2 + 4\tau(2\gamma_0\lambda - C_{\varphi,q})} - \gamma}{4\tau}. \tag{14}$$

Inserting these values in Eq. (8) for the parameters used in our simulations, the minimisation of the noise sum yields $\tau_{opt} \approx 0.2$ (see Fig. 4).

Quantum hysteresis is not pinched at 0

In the unconditioned evolution of the quantum memristor, the $\langle\langle q\rangle\rangle$ vs. $\langle\langle \gamma(\mu) q\rangle\rangle$ curve is not necessarily pinched at the origin. In fact, numerically evaluating the deviation from factorisation $\delta_q = \langle\langle \gamma(\mu) q\rangle\rangle - \langle\langle \gamma(\mu)\rangle\rangle\langle\langle q\rangle\rangle$, provided small ($\leq 0.1$), but non-zero values for the zero crossings of $\langle\langle q\rangle\rangle$. The resulting hysteresis observed in the unconditioned evolution is depicted in Fig. 5. Due to the correlations between damping rate and charge on the capacitor, this corresponds to non-zero (quantum average) current for vanishing (quantum average) voltage. The passivity of the device is still guaranteed, as the expectation value of the emitted power fulfils $\langle\langle I_M V\rangle\rangle \propto \langle\langle \gamma(\mu) q^2\rangle\rangle \geq 0$.

Noisy signals and hysteresis

Both noisy voltage signals and fluctuations of the state variable have been studied for classical memristors [8, 23]. However, for a classical voltage signal, these two noise sources are independent and can be simultaneously suppressed, whereas in the quantum case of the measurement back-action ties them together. The parameter that controls the noise amplitude is the measurement strength k, or more precisely, the projection frequency $\tau = q_0^2 k$, as defined in the main text. For a strong measurement, (large $\tau \gg 1/\omega_0$), noise in the state variable is suppressed, but the back-action increases the fluctuations in the first moments of flux and charge, thus leading to diffusion of the state variable. On the contrary, for a weak measurement, $\tau \ll 1/\omega_0$, first moments evolve in an almost unperturbed manner, but the loss of information in the voltage measurement produces a highly fluctuating state variable update. Finally, the accumulated noise has to be compared to the typical charge on the capacitor, q_t, which represents the signal to be recorded, and the threshold 2π, from which on hysteresis collapses. As a Wiener noise contribution of the form $D\mathrm{d}W$ induces a linear growth in time of the variance proportional to Dt^2, the condition for the existence of hysteresis up to a time t_C reads (in adimensionalized terms)

$$8\tau V_q t_C, 8\tau C_{\varphi,q} t_C, \frac{t_C}{8\tau} \ll \min(q_t^2, 4\pi^2). \tag{15}$$

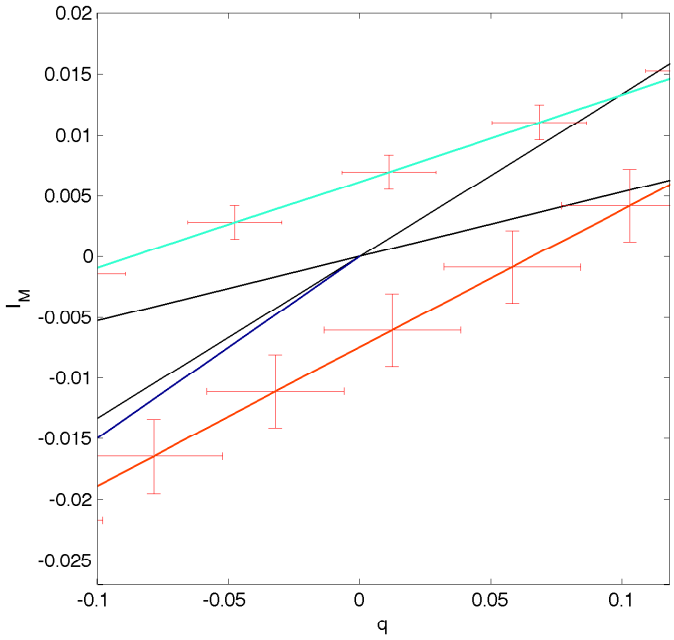

FIG. 5. Blow-up of the region around the origin of Fig. 2a revealing non pinching at the origin.This is due to the deviation $\delta_q(t)$ from factorisation of $\langle\langle\gamma(\mu)q\rangle\rangle$. Only one and a half oscillations are shown, for clarity. The black line corresponds to the classical I-V curve. The red bars denote the ensemble estimation error, not including numerical errors due to the Euler Algorithm.

Like all open quantum systems, a quantum memristor is subject to decoherence, a process which has been extensively studied in the context of the quantum-to-classical transition [24]. However, a memory-specific feature of the memristive environment consists in the continuous monitoring of the system with a fine-tuned measurement strength. It is known that continuous measurements are able to provide well-localised trajectories in phase space, a characteristic of classical systems [25]. In a linear system, such as the LC circuit, the measurement strength has to fulfil two conditions in order for localisation of trajectories to take place, namely, sufficient suppression of the variances and a negligible measurement back action in comparison to the system dynamics. The amplitude of the system dynamics is given by the typical action of the system s (in units of $\hbar$) and constraints the projection frequency by [25, Eq. (6)],

$$\frac{2}{s} \ll \tau \ll 4s. \tag{16}$$

The typical action can be estimated by $s = \frac{\langle E\rangle}{\hbar\omega_0} \approx q_t^2$ (with charge unit q_0) and therefore the conditions in Eq. (15) for a memory effect coincide with the requirement for a well-localised trajectory. Loosely speaking, a localised phase space trajectory keeps the state variable localised as well, and thus allows for memory effects.

In order to connect the requirement for a memory effect up to time t_C in Eq. (15) and the condition for a well-localised phase space trajectory in Eq. (16), we first concentrate on fluctuations of first moments. The noise in the first moments induced by the measurement becomes important for large measurement strengths, say $\tau > 1/\omega_0$. In this regime, and using the adimensional setting of the main text, the noise is dominated by the term $\sqrt{8\tau}C_{\varphi,q}$ with $C_{\varphi,q} \approx \frac{1}{2}$ and hence the first two inequalities in Eq. (15) require

$$\frac{8\tau t_C}{2} \ll q_t^2.$$

This corresponds to the upper bound for the projection frequency in Eq. (16) growing linearly with the typical action s in units of the planck constant, because $s = \frac{\langle E\rangle}{\hbar\omega} = \frac{q_0^2}{\hbar\omega C} q^2 = q^2$. Correspondingly, the last inequality in Eq. (15)

$$\frac{t_C}{8\tau} \ll q_t^2 \Rightarrow \frac{t_C}{8q_t^2} \ll \tau \tag{17}$$

provides the inverse scaling with the typical action s of the lower bound on τ in Eq. (16).

Numeric implementation

We study Gaussian state dynamics in an LC circuit coupled to a quantum memristor with numerical simulation of the set of equations (8). These are stochastic differential equations with Gaussian noise and are cast in Itô form. We use the explicit Euler algorithm [2, ch.10]. It is based on the discretisation of the equations according to

$$\begin{aligned} \mathrm{d}t &\to \Delta t, \\ \mathrm{d}W &\to G\sqrt{\Delta t}, \end{aligned}$$

where Δt has to be chosen sufficiently small and the G are independently, identically, distributed values drawn from a Gaussian distribution with mean 0 and variance 1.

Concretely, the simulation is implemented in Matlab (code available upon request). All the above results are obtained with a time increment $\Delta t = 10^{-3}$, which in the chosen units is much smaller than the period of one oscillation in the LC circuit, $T = 2\pi$. In order to obtain the hysteresis curves of the ensemble we average over 3000 trajectories.

The stability of our implementation with respect to the choice of the time increment and the sufficient ensemble size is demonstrated by a comparison of the evolution of the damping rate $\gamma(\mu(t))$ for different time increments in Fig. 6. Furthermore, we have also carried out a simulation using the inbuilt version of the Euler algorithm in Mathematica, and, qualitatively, the behaviour is the same. In fact our implementation is more stable for longer times, because of the poor handling of large ensemble sizes in the version of Mathematica available to us.

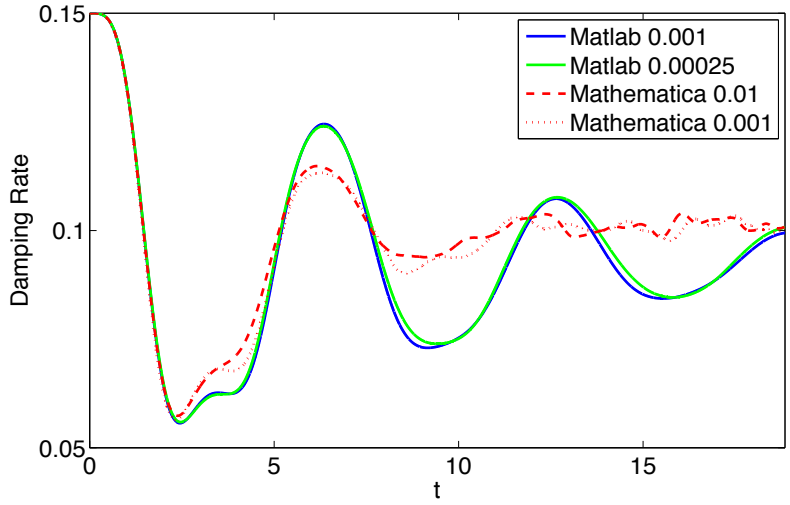

FIG. 6. Test of the Matlab code via a comparison of the evolution of the mean value damping rate with a solution obtained in Mathematica. The different lines depict different time increments $\mathrm{d}t$. The ensemble sizes are: 3000 (Matlab), 300 (Mathematica).